Contemporary Engineering Sciences, Vol. 9, 2016, no. 17, 823 - 834
HIKARI Ltd, www.m-hikari.com
http://dx.doi.org/10.12988/ces.2016.66115

Experimental Investigation of Air-Water HPHE Using Ethanol as the Working Fluid

Y. Pakam and T. Soontornchainacksaeng

Department of Mechanical and Aerospace Engineering, Faculty of Engineering
King Mongkut's University of Technology North Bangkok
Bangkok, 10800, Thailand

Abstract

This research reported the analytical model and experiment of air-water Heat Pipe Heat Exchanger (HPHE). HPHE comprised of 13 vertical-staggered heat pipes 12.7 mm stainless steel heat pipe 320 mm in length and stainless steel-plate fins 2 mm in thickness. Ethanol-charged HPHE contained the screen wick had an evaporation of 150 mm, a condensation of 150 mm and adiabatic of 20 mm. HPHE was analyzed the counter flow effect of temperature for inlet hot air, 100-140°C, and mass flow rates, 180 and 230 LPM, with constant water's temperature, 30°C, and flowrate ranges, 0.25 to 0.75 LPM. MATLAB simulated the temperature for outlet water, the heat transfer rate and thermal effectiveness differed from the experiment results within 4.00%, 15.13% and 12.66% respectively. Finally, the temperature for inlet hot air 140°C and AHCR:WHCR = 0.22 gave the best at 45.90°C. In contrast, AHCR:WHCR = 0.06 gave the best thermal effectiveness 0.91.

Keywords: Heat pipe heat exchanger, Thermal recovery applications, Heat transfer rate, Screen wick, Ethanol

1 Introduction

Heat Pipe Heat Exchanger (HPHE) is one of applications recovering thermal from a hot stream fluid to a cold stream fluid. HPHE consists of the evaporation zone, adiabatic zone and condensation zone. Heat source transferred to each heat pipe boils the working fluid that changes the phase from liquid to vapor going up to the top. Then it releases the heat to cold stream fluid at the condensation zone. The working fluid condenses to liquid phase flowing via the wick and to the evaporator

zone to be heated again [1] as shown in figure 1. HPHE are applied many of systems in which a hot stream fluid and a cold stream are not be mixed such as economizer in boiler, cooling device in CPU, heat exchanger device in air-conditioning and heat recovery in engine etc. There are many of studying on the HPHE in Laboratory. For instance, the theoretical model for water-charged HPHE provided in an air to water was investigated with the experimental results in the heat transfer rates and the effectiveness [2]. Next, the mathematic models for sodium-charged HPHE were created to predict the thermal performance with the high temperatures for inlet hot air and the low temperatures for inlet water [3] as well as the steel HPHE was investigated with experiment results in case of hot air exchanging the temperatures with a constant flowrate for cool water. [4]. Some researches focused on air conditioning system, the calculation program was established to predict the heat recovery values respecting the inlet ambient air in the air compressor 1 kg/TR. [5]. Furthermore, HPHE also applied to vehicles [6]. And, it also was in the form of thermoelectric generators by which can reduce fuels and emissions [7]. For the refrigeration system, there was the HPHE used R134a as the working fluid to reduce moisture for the inlet air [8]. And, using HFC134a and HFO1234ze (E) as the working fluid for the air conditioning system [9]. Moreover, there was the heat recovery of an exhaust gas to exchange with a cold water in the pasteurized dairy process [10]. In addition, there were the researches of heat transfer mechanism inside the heat pipe. Screen wick in heat pipe tested to know the phenomenon was provided the mathematic models to predict the dry out limit [11] as well as screen wick was tested the maximum heat transfer rates [12].

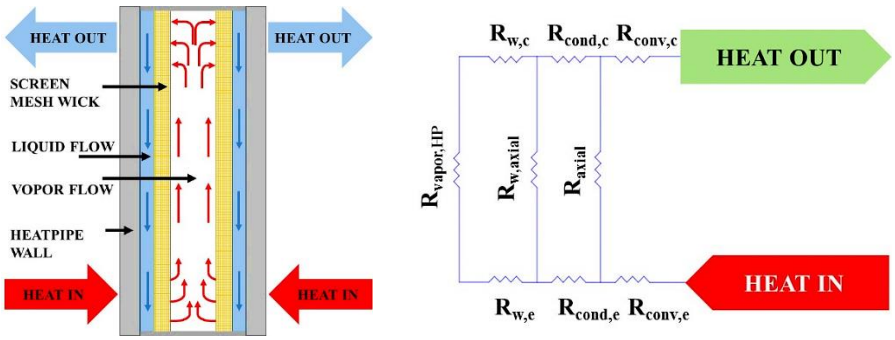

Figure 1 shows the thermal cycle in heat pipe

Regarding the above literature review, this research are reported the experimental and theoretical investigation of a 13-staggered HPHE. The ethanol-charged HPHE are vertical stainless steel with plate fins. HPHE operating with inlet hot air at evaporation zone exchanges with inlet water. The analytical models are investigated with the experimental results. This research is expected to obtain the information to develop the HPHE's design further.

2 Materials and Methods

2.1 Governing equations of HPHE

The average heat transfer coefficient of HPHE is very importance for hot air and water flowing via the heat pipes bank [13]. As the HPHE is placed with the staggered arrangement as shown in figure 2. Firstly, the maximum Reynold number is the function of maximum velocity, diameter, dynamic viscosity and density. The maximum velocity is the flowing fluid via the smallest channel between two heat pipes at the same row [14], [15]. Thus, The Nusselt number is generally a function of the maximum Reynolds number, Re_{max}, the Prandtl number, Pr. Diameter of heat pipe, d, the transverse distance between two consecutive tubes, S_T, and the longitudinal distance between two consecutive tubes, S_L. Then Nusselt number can be expressed by equation 1

$$Nu_{HPHE} = \frac{1+(n-1)f_A}{n}\left(0.3+\sqrt{(0.664\sqrt{Re_{max}}Pr^{1/3})^2+(\frac{0.037Re_{max}^{0.8}Pr}{1+2.433Re_{max}^{-0.1}(Pr^{2/3}-1)})^2}\right) \quad (1)$$

Where n is the number of heat pipe rows and f_A which is the arrangement factor [16]. Therefore, the mean heat transfer coefficient can be obtained by equation 2

$$\bar{h} = \frac{Nu_{HPHE}k}{d} \quad (2)$$

Where k is the thermal conductivity of material. Furthermore, HPHE is also installed the plate fins to increase the surface area. Then the overall surface efficiency η_o for a plate fin concerned about the hexagonal fin lay out as shown in figure 2 can be defined by equation 3 [17].

$$\eta_o = 1-\frac{N_{fin}A_{fin}}{A_{HPHE}}\left(1-\frac{tanh\left(\sqrt{2\bar{h}/k\delta}\,\frac{S_T}{\sqrt{3}}\left(\frac{2S_T}{\sqrt{3}d}-1\right)\left(1+0.35ln\left(\frac{2S_T}{\sqrt{3}d}\right)\right)\right)}{\left(\sqrt{2\bar{h}/k\delta}\,\frac{S_T}{\sqrt{3}}\left(\frac{2S_T}{\sqrt{3}d}-1\right)\left(1+0.35ln\left(\frac{2S_T}{\sqrt{3}d}\right)\right)\right)}\right) \quad (3)$$

Where the S_T is the transverse distance between two consecutive tubes, the N_{fin} is the number of plate fin, the A_{fin} is the surface area of plate fin, the A_{HPHE} is the surface area of HPHE, and δ is the plate fin's thickness.

The heat transfer of heat pipe contains the thermal conductivity at the wall and screen wick. The screen wick's thermal conductivity, $k_{l\text{-}wick}$, can be determined by equation 4 [18] and [19].

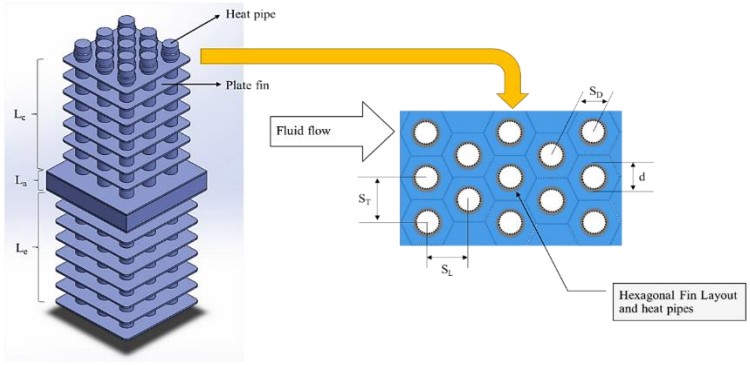

Figure 2 Schematic of staggered HPHE and plate fins

$$k_{l\text{-}wick} = \frac{k_l[(2k_l + k_{wick}) - (1-\varphi)(k_l - k_{wick})]}{(k_l + k_{wick}) + (1-\varphi)(k_l - k_{wick})} \tag{4}$$

Where k_l, k_{wick} and φ is the working fluid's thermal conductivity at liquid state, the material's thermal conductivity and the screen wick porosity respectively. Where porosity of the screen wick which is the function of wick diameter, d_{wick}, and layer of wick, ς, can be calculated by $\varphi = 1 - 1.05\pi d_{wick}/\varsigma$ [18]. In the thermal analysis need to evaluate the overall heat transfer coefficient, U. Then it can be expressed by equation 5 [20]

$$U = \frac{1}{\left(\sum_{n=1}^{n=8} R_n\right) A_{HPHE}} \tag{5}$$

Where R_n is combination of the thermal resistance as shown in figure 2. Finally, the heat transfer rates can be determined by equation 6

$$q = UA_{HPHE}\Delta T \tag{6}$$

The flow across the staggered arrangement heat pipes, the surface temperatures of heat pipe of evaporation and condensation zone are uniformed. Thus the log mean temperature different can be estimated by equation 7

$$T_{out} = T_s - (T_s - T_{in})exp\left(-\frac{A_{HPHE}\bar{h}}{\rho_f u_m (YZ - N_{fin}\delta Z_{fin})c_{p,f}}\right) \tag{7}$$

Where the T_{in} and T_{out} is the inlet and outlet temperature of fluids. And, the ρ_f is the density of fluid. Next, the Y and Z is the high and with of channel for evaporation zone and condensation zone respectively. The Z_{fin} is the fin's width and $c_{p,f}$ is the heat capacity of fluid. For the thermal effectiveness of the HPHE that can be determined by equation 8

$$\varepsilon = \frac{C_h(T_{h,in} - T_{h,out})}{C_{min}(T_{h,in} - T_{c,in})} = \frac{C_c(T_{c,out} - T_{c,in})}{C_{min}(T_{h,in} - T_{c,in})} \tag{8}$$

Where the C_h is the hot air heat capacity rates, and the C_c is water heat capacity rate. Then, the C_{min} is minimum fluid heat capacity rate.

2.2 Computational procedure

For the hypothesis of the governing equations, the hot air and water was assumed to be incompressible with constant property and its flow was in steady state condition. Moreover, these were not considered in kinematic energy, potential energy, thermal resistance occurring at the vapor-liquid interface, axial thermal resistance of wick and solid wall as well as uniform surface temperature of the heat pipes. Regarding the calculation by MATLAB. In order to input the parameters, the physical of HPHE and the properties of fluids as well as the working fluid must be put. Next, the temperatures for inlet hot air and inlet water are then put as well in order to calculate all of thermal resistance as equation 5, but the thermal resistance occurring at the vapor-liquid interface was not computed in this step. Then, the heat transfer rate was guessed to compute the thermal resistance occurring at the vapor-liquid interface that was combined with the other thermal resistances. The heat transfer rate was iterated through computer program until its consistency, ≤ 0.001. After that, heat transfer rate was conducted to calculate the surface temperature both evaporation zone and condensation zone. Due to the staggered arrangement, the odd row and even row of surface area were different. Thus, the mathematic codes of temperature for both of outlet hot air and outlet water defined the conditions must be concerned until the complete rows were computed the outlet temperature for hot air and water. As the figure 3, the effectiveness could be determined.

2.3 Experiment apparatus and Experimentation

The main equipment of apparatus comprised of a HPHE, a hot air blower heater, a water basin, a cold water pump, a water Rota meter, anemometer and a data collecting system, etc. In case of the counter-flow HPHE, hot air entered to the evaporation zone and cold water entered to the condensation zone. The ethanol-charged HPHE comprised of 13 vertical-staggered heat pipes 12.7 mm stainless steel heat pipe 320 mm in length and stainless steel-plate fins 2 mm in thickness. Each of heat pipe which charged ethanol as working was contained the screen wick

and had an evaporation zone of 150 mm, a condensation zone of 150 mm and adiabatic zone of 20 mm. Moreover, each of heat pipe contained screen mesh, stainless steel no.100. Hot air generated the high temperature by air blower heater, Leister - model: 142.609, flowed via the evaporation zone. And, air velocity was measured by a digital anemometer. Water was transferred by pump with constant temperature from water basin via condensation zone. The temperatures measured by thermocouples K-type were recorded by data collecting system transferred to computer with Primus program as shown in figure 4.

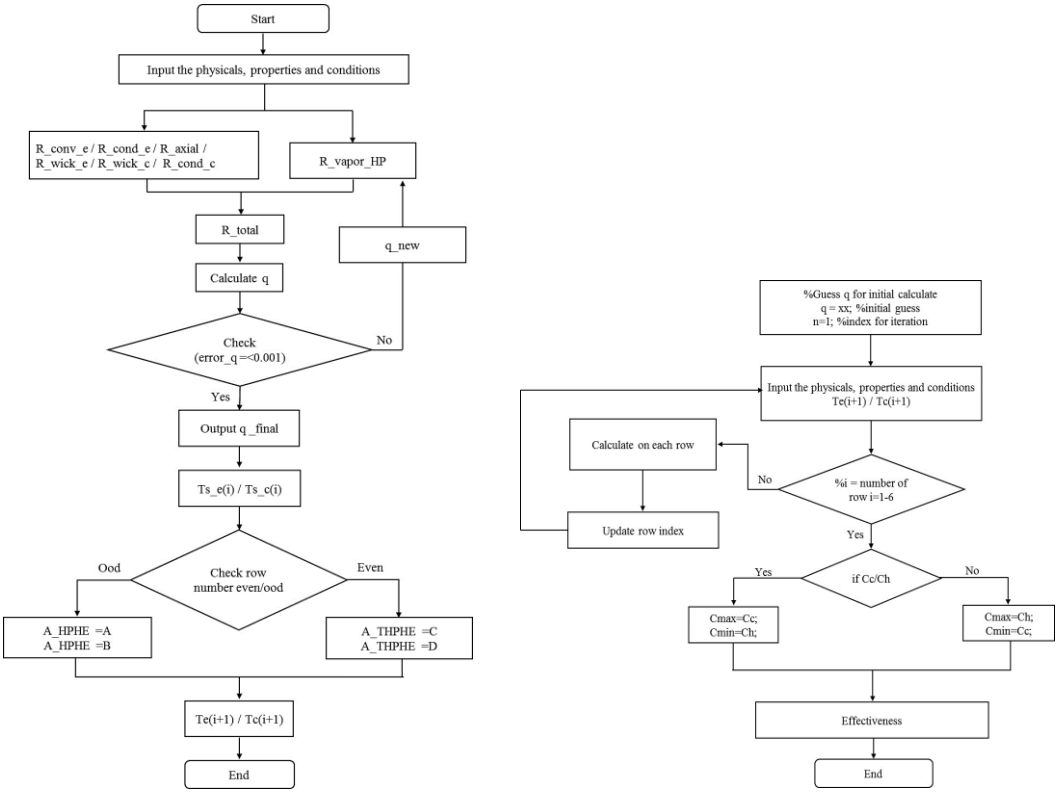

Figure 3 shows the Flow chart of numerical simulation

For the experiment of HPHE, The inlet hot air set the temperature at 100 to 130˚C entered with flowrate 180 and 230 LPM. For the inlet water set the constant temperature 30.0±2.0˚C entered with flowrate 0.25 to 0.75 LPM. The thermodynamic properties of hot air is different from that of water. For the hot air, the density is 0.850 kg/m3 and the isobaric specific heat capacity is 1.013 kJ/(kg K). For the water, the density is 990 kg/m3 and the isobaric specific heat capacity is 4.179 kJ/(kg.K). All data were calculated for the outlet temperature for fluids, heat transfer rates and effectiveness with thermodynamics and heat transfer principles. This experiment was tested at the ES-MVC Center, Science and Technology Research Institute, King Mongkut's University of Technology North Bangkok, Thailand as figure 4.

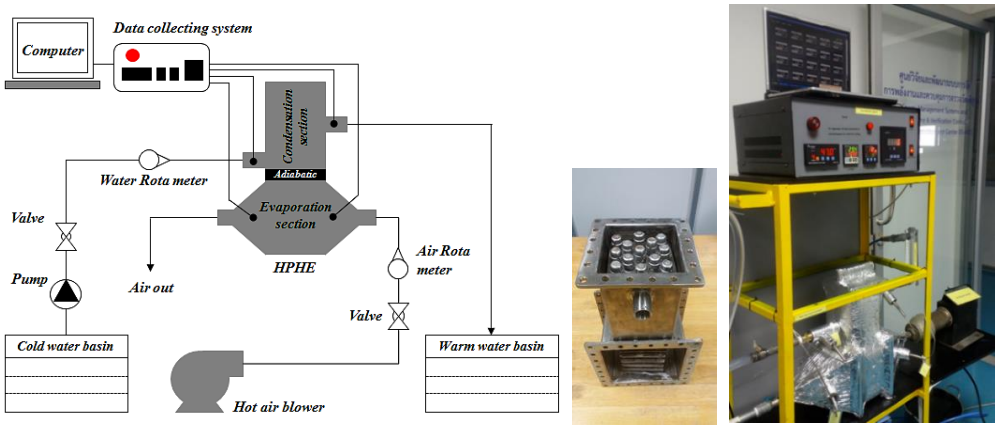

Figure 4 shows the schematic view of the HPHE and Photos

3. Results and Discussion

3.1 Verifying the analytical models

Before analytical model was investigated with experiments, it was verified with H. Zare Aliabadi's results. Especially, in the conditions that the temperature for inlet hot air at 125°C and for inlet water at 17°C and the hot air heat capacity rates to water heat capacity rates (AHCR:WHCR) was the range 0.420 to 1.266. The analytical model results for outlet temperatures were reported as follows; the outlet temperatures for hot air were likely to the same trend as verified research, when the AHCR:WHCR and the temperatures for inlet hot air were increased, the temperatures for outlet hot air increased as well. The lowest-outlet temperature was the AHCR:WHCR = 0.42 but the highest-outlet temperature was the AHCR:WHCR = 1.266. From the verification results showed that the analytical model was lower than the simulations average 3.70%, and was higher than the experiments average 3.04%. Next, the heat transfer rates showed the trend that was similar to the verified research when the AHCR:WHCR was increased, the heat transfer rate increased every temperature for inlet hot air as well. As the matter of fact, the results of analytical models showed the range from 12,917 to 23,511 Watt. Then, the analytical model results were higher than the simulations average 5.38% as well as the experiments average 7.89%. As shown in the figure 5, the effectiveness was similar to verified results. When the AHCR:WHCR = 1.0, the thermal effectiveness was the lowest at 0.42. In contrast, the AHCR:WHCR > 1.0 carried out the rising thermal effectiveness up again. Thus, the analytical model was lower than the simulations average 5.66%, and was higher than the experiments average 8.20%. After verification, the staggered arrangement was more thermal effectiveness than the in-line arrangement. Finally, the analytical model could be applied to other materials, and other conditions appropriately.

3.2 Temperature for outlet water

In case of the temperature for outlet water, the experiment results showed in figure 6. The temperatures for inlet hot air 100 to 140°C and the AHCR:WHCR ranges 0.06 to 0.22 had the temperature for outlet water 34.00 to 45.90°C. Thus, the temperature for inlet hot air 140°C and AHCR:WHCR = 0.22 gave the best at 45.90°C. Moreover, the error of analytical model was less than the experiment results average 4% as shown a couple temperatures for inlet hot air in figure 6.

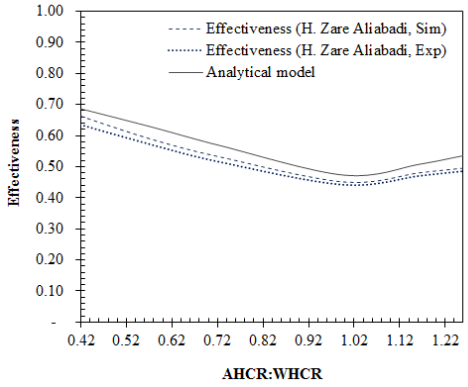

Figure 5. shows the verified thermal effectiveness

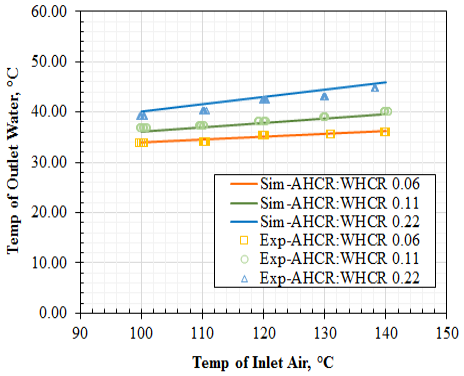

Figure 6. shows the comparison of simulation and experiment

3.3 Heat transfer rates

Regarding the analytical model and experiment investigation. Considering the heat transfer rate of water, the experiment results showed in figure 7. The temperatures for inlet hot air 100 to 140°C and the AHCR:WHCR ranges 0.06 to 0.22 had the heat transfer rates 142.78 to 308.20 W. Thus, the temperature for inlet hot air 140°C and AHCR:WHCR = 0.06 gave the best heat transfer rate at 308.20 W. Moreover, the analytical model was higher than the experiment results average 15.13% as shown a couple temperatures for inlet hot air in figure 8.

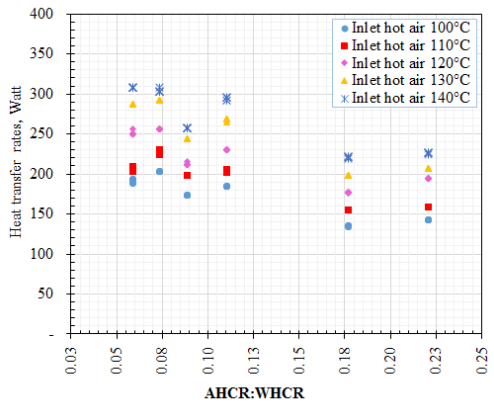

Figure 7. shows the heat transfer rates varying temperature for inlet hot air and AHCR:WHCR

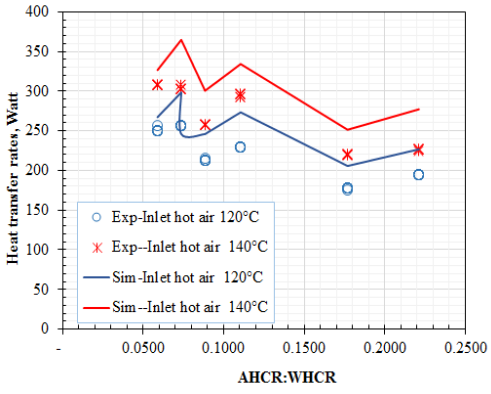

Figure 8. shows the comparison between simulation and experiment varying temperature

3.4 Thermal Effectiveness

For the effectiveness investigation, the experiment results showed in figure 9. The temperatures for inlet hot air 100 to 140°C and the AHCR:WHCR ranges 0.06 to 0.22 had the thermal effectiveness 0.54 to 0.91. Thus, the temperature for inlet hot air 140°C and AHCR:WHCR = 0.06 gave the best thermal effectiveness 0.91. Moreover, the analytical model was higher than the experiment results average 12.66% as shown a couple temperatures for inlet hot air in figure 10.

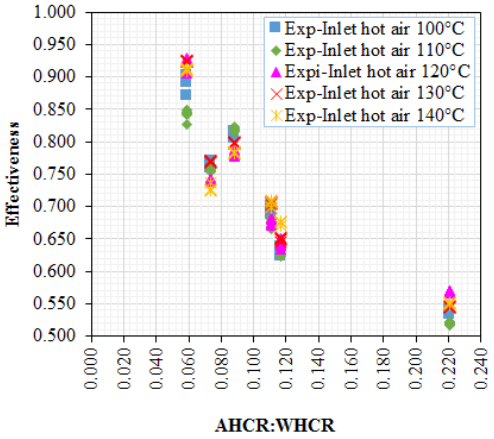

Figure 9. shows the thermal effectiveness varying temperature for inlet hot air and AHCR:WHCR

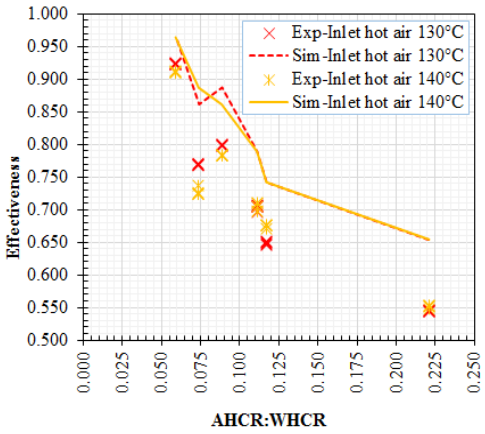

Figure 10. shows the comparison between simulation and experiment at inlet hot air temp. 130 and 140°C

4. Conclusions

This report indicated the ethanol-charged HPHE concerning the temperature for outlet water, heat transfer rate and thermal effectiveness. The HPHE was experimentally tested to investigate the analytical model which closed to the verified research in temperature distributions, heat transfer rate and thermal effectiveness less than 10%. Furthermore, the analytical model compared with experiment results could be explicated the conclusions as follows:

- Temperature for outlet water, the temperature for inlet hot air 140°C and AHCR:WHCR = 0.22 gave the best at 45.90°C. And, the error of analytical model was less than the experiment results average 4%
- Heat transfer rates, the temperature for inlet hot air 140°C and AHCR:WHCR = 0.06 gave the best heat transfer rate at 308.20W. And, the analytical model was higher than the experiment results average 15.13%
- Thermal effectiveness, the temperature for inlet hot air 140°C and AHCR:WHCR = 0.06 gave the best thermal effectiveness 0.91. And, the analytical model was higher than the experiment results average 12.66%

Thus, this analytical model can be applied to design the HPHE in further.

Acknowledgments. This research was supported by Energy Management Systems and Monitoring & Verification Control (ES-MVC), Science and Technology Research Institute, KMUTNB

References

[1] D.A. Reay and P.A. Kew, *Heat Pipe, Theory, Design and Application*, Elsevier, Burlington, 2006.

[2] H. Zare Aliabadi, H. Ateshi, S.H. Noei and M. Khoram, An Experimental and Theoretical Investigation on Thermal Performance of a Gas-Liquid Thermosyphon Heat Pipe Heat Exchanger in a Semi-Industrial Plant, *Iranian Journal Chemical Engineering*, **6** (2009), 13-25.

[3] R. Laubscher and R.T. Dobson, Theoretical and experimental modelling of a heat pipe heat exchanger for high temperature nuclear reactor technology, *Applied Thermal Engineering*, **61** (2013), 259-267. http://dx.doi.org/10.1016/j.applthermaleng.2013.06.063

[4] H. Mroue, J.B. Ramos, L.C. Wrobel and H. Jouhara, Experimental and numerical investigation of an air-to-water heat pipe-based heat exchanger, *Applied Thermal Engineering*, **78** (2015), 339-350. http://dx.doi.org/10.1016/j.applthermaleng.2015.01.005

[5] T.S. Jadhav and M.M. Lele, Theoretical energy saving analysis of air conditioning system using heat pipe heat exchanger for Indian climatic zones, *Engineering Science and Technology, an International Journal*, **18** (2015), 669-673. http://dx.doi.org/10.1016/j.jestch.2015.04.009

[6] F. Yang, X. Yuan and G. Lin, Waste heat recovery using heat pipe heat exchanger for heating automobile using exhaust gas, *Applied Thermal Engineering*, **23** (2002), 367-372. http://dx.doi.org/10.1016/s1359-4311(02)00190-4

[7] R. Saidur, M. Rezaei, W.K. Muzammil, M.H. Hassan, S. Paria and M. Hasanuzzaman, Technologies to recover exhaust heat from internal combustion engines, *Renewable and Sustainable Energy Reviews*, **6** (2012), 5649-5659. http://dx.doi.org/10.1016/j.rser.2012.05.018

[8] A. Meyer and R.T. Dobson, A heat pipe heat recovery heat exchanger for a mini-drier, *Journal of Energy in Southern Africa*, **17** (2006), 50-57.

[9] G.A. Longo, G. Righetti, C. Zilio, F. Bertolo, Experimental and theoretical analysis of a heat pipe heat exchanger operating with a low global warming potential refrigerant, *Applied Thermal Engineering*, **65** (2014), 361-368. http://dx.doi.org/10.1016/j.applthermaleng.2014.01.023

[10] S. Niamsuwana, P. Kittisupakorna and I. Mujtabab, A newly designed economizer to improve waste heat recovery: A case study in a pasteurized milk plant, *Applied Thermal Engineering*, **60** (2013), 188-199. http://dx.doi.org/10.1016/j.applthermaleng.2013.06.056

[11] T.S. Liang and Y.M. Hung, Fabrication of composite wick structure heat spreader, *Journal of Marine Science and Technology*, **20** (2012), 158-162.

[12] K. Hiroaki, I. Hideaki and I. Yuji, The permeability of screen wicks, *The Japan Society of Mechanical Engineers (JSME)*, **34** (1991), 212-219.

[13] J.G. Knudsen and D.L. Katz, *Fluid Dynamics and Heat Transfer*, Chemical Engineering Series, McGraw-Hill, 1958.

[14] W.A. Khan, J.R. Culham and M.M. Yovanovich, Convection heat transfer from tube banks in crossflow: Analytical approach, *International of Heat and Mass Transfer*, **49** (2006), 4831-4838. http://dx.doi.org/10.1016/j.ijheatmasstransfer.2006.05.042

[15] V.K. Mandhani, R.P. Chabra and V. Eswaran, Forced convection heat transfer in tube banks in cross flow, *Chemical Engineering Science*, **57** (2002), 379-391. http://dx.doi.org/10.1016/s0009-2509(01)00390-6

[16] B.M. Brienza, J.B. Gandy and L.L. Gonzalez, *Heat Exchanger Design Handbook*, heat and mass transfer, Book Crafters, 1983.

[17] M.F. Wright, *Plate – Fin and- Tube Condenser Design for Refrigerant R-410 Air-Conditioner*, Georgia Institute of Technology, Georgia, 2000.

[18] A.B. Solomon, K. Ramachandran, L.G. Asirvatham and B.C. Pillai, Numerical analysis of a screen mesh wick heat pipe with Cu/water nanofluid, *International Journal of Heat and Mass Transfer*, **75** (2014), 523-533. http://dx.doi.org/10.1016/j.ijheatmasstransfer.2014.04.007

[19] L.L. Jiang, Y. Tang, W. Zhou, L.Z. Jiang, T. Xiao, Y. Li and J.W. Gao, Design and fabrication of sintered wick for miniature cylindrical heat pipe. *Transactions of Nonferrous Metals Society of China*, **24** (2014), 292-301. http://dx.doi.org/10.1016/s1003-6326(14)63060-0

[20] F.P. Incropera and D.P. Dewitt, *Fundamentals of Heat and Mass Transfer*, John Wiley, New York, 2002.

Received: July 8, 2016; Published: August 11, 2016